Journal of Engineering and Technology for Industrial Applications

ISSN ONLINE: 2447-0228

ITEGAM-JETIA

Manaus, v.11 n.54, p. 131-139. July/August., 2025.

DOI: https://doi.org/10.5935/jetia. v11i54.2118

RESEARCH ARTICLE OPEN ACCESS

DEVELOPMENT AND VALIDATION OF A MULTI-SOURCE BRIDGE DC–DC CONVERTER FOR EV APPLICATIONS

Baya Reddy Lomada[1], V. Naga Bhaskar Reddy[2]

[1]Research scholar, Dept of EEE, JNT University, Anantapur, Andhra Pradesh, India.
[2] Professor,Senior member IEEE, Dept of EEE RGMCET, Nandyal, Andhra Pradesh, India.

[1]https://orcid.org/0000-0002-8396-9882, [2]https://orcid.org/0000-0002-3073-9565

Email: reddy.baya@gmail.com, nagabhaskarreddy@rgmcet.edu.in

ARTICLE INFO

Article History
Received: June 28, 2025
Revised: July 13, 2025
Accepted: June 15, 2025
Published: July 31, 2025

Keywords:
Mathematical modeling
DC-DC converter
Validation
Multi-Input Converter
Hybrid energy system

ABSTRACT

As per the current scenario of exhausting the oil supplements across the globe because of rapid increase in the consumption of conventional resources which causes the destruction of environment and human life as they emit CO2, SO2 and oxides of nitrogen gas. Hybrid Electric Vehicle (HEV) plays vital role now a days to overcome the above hazards. This article provides a detailed investigation of a multi-input DC converter (MIC) including its mathematical modelling, design, validation of the prototype, and analysis. This converter actively accepts solar photovoltaic (PV) panels and fuel cells as sources. Converter achieve broad control of output voltage and power flow with help of multiple switching frequencies. The steady-state modeling are demonstrated to achieve accurate design and analysis. The recommended converter assurances reduced stress on voltage, fewer switches, and fewer circuit components while offering higher gain and 96.4% efficiency.

I. INTRODUCTION

A surplus of energy sources are being exploited to meet the rising demand for power [1-3]. The world's expanding need for electricity can no longer be met by traditional energy sources since they are quickly running out [4]. The use of natural fuels for energy production also has a detrimental effect on the environment, raising concerns about things like air pollution and global warming [5]. The output of electricity derived from renewable energy sources is consequently rising swiftly, particularly in distributed generation [6]. Thus, developing hybrid energy plans that continuously supply power to the right demand through a variety of green technologies is crucial [7]. The huge majority of EV are battery powered, which depends on two important variables: the availability of lithium and the state of the electricity network today [8].

To avoid the issues, research and tests on fuel cell-based cars, photovoltaic and fuel cell hybrid electric cars must be carried out concurrently [9]. For such cars, the paucity of lithium and the contemporary power grid are irrelevant. Hydrogen best compares to batteries in terms of both energy density and power density [10]-[12]. Because hydrogen is expensive, it is perfect to use PV panels in addition to fuel cells to reduce the useage of hydrogen in the vehicle [13], [14]. As shown in Figure. 1, the solar PV, fuel cell, inverter, multi-input DC-DC converter & electric motor comprise the primary powertrain components of HEV. A multi-input DC-DC converter has a substantial impact on the overall stability and functionality of the HEV powertrain system. Experts have created many MICs, but not all of them are appropriate for every application compared to non-isolated MICs, other types of MICs are far fewer useful for slight and medium-powered HEVs.

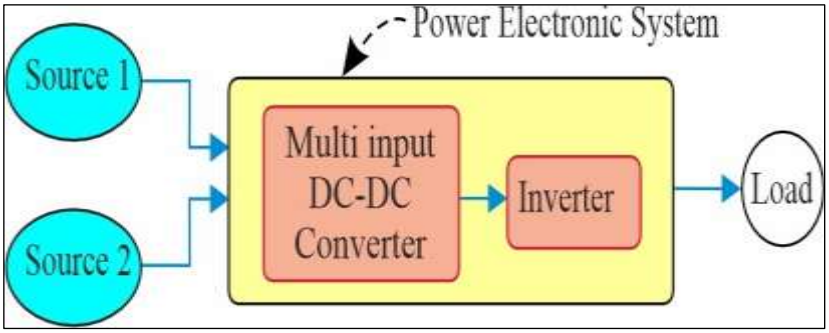

Figure 1: Block diagram of HEV.
Source: Authors, (2025).

A novel MIC configuration developed with the basic single-ended primary-inductor converter (SEPIC) was presented by the researchers in [15]. It is feasible to integrate many inputs, but at least one of them must be a rechargeable battery. Regretfully, there is a great deal of voltage stress on the switching electronics. A unique MIC structure is described in [16] to integrate the super-capacitor and rechargeable battery for EVs. Relays are used in this converter to carry out the required function no need any additional circuity for one input can feed the other which comparatively increases the circuit difficulty. In Experts in [17]. The authors of [18] introduced a novel type of MIC bridge for establishing connections between many renewable energy sources. To get a larger gain, fewer unidirectional and bidirectional semiconductor switches are used. Depending on the number of switches operating in each mode, the stress placed on each switch in this architecture increases. Furthermore, a polarity change between the input and output voltages is seen. A bidirectional MIC was described by the authors of [19].

This work is primarily focused on calculating critical inductance and minimizing voltage ripple. Although there are more switching components and a battery input required, this converter can give electricity in both directions. The development and analysis of a MIC are shown in the article [20]. Reducing the number of Components and the stress on the switch voltage are the converter's key concerns. Unfortunately, there are more losses in this converter, and there are still a lot of components. In [21], A unique modular MIC was suggested by the researchers. It has slight components, a smaller amount of voltage stress, and a better voltage gain. Nevertheless, there are more parts in this converter, and several switches are under more voltage stress. It also uses a more of storage components for a multi-input system, which complicates control design and system analysis. In [22], A non-isolated MIC for RES was presented by the authors. Due to the non-coupled inductor, this converter shows greater gain on voltage at a fewer component count... In [23], the authors presented a Multi-Input High Gain Non-isolated DC–DC Converter with a new design and a condensed component. One diode is utilized to enable bidirectional power flow in order to reduce the number of components and create high voltage gain.

II. PROPOSED CONVERTER

The working principle of the MIC and traditional converters is quite similar. In both cases, the inductive and capacitive components of the converter charge for a predetermined amount of time and then dis-charge through a load for the rest period of time. The operating technique is the same in the suggested converter. Figure. 2 illustrates the recently built MICs intended for HEV use.

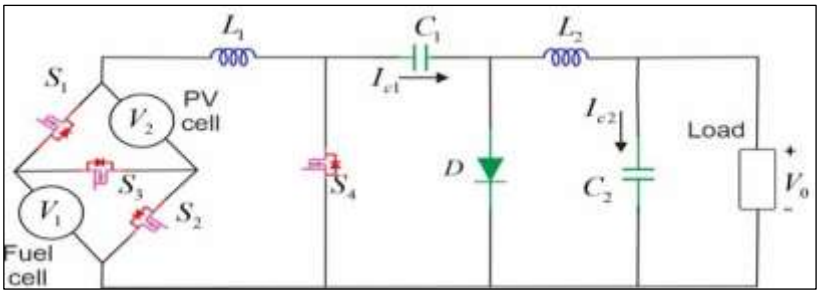

Figure 2: shows the suggested converter structure.
Source: Authors, (2025).

II.1 MODES OF OPERATION

Figure. 3 shows the equivalent circuitry for the six modes of operation of the suggest converter. In Figure. 2, fuel cell voltage is V_1, the solar panel output voltage is V_2, S_1 to S_4 are the four MOSFET switches, D is the diode, R is the load resistance, two inductors are L_1 and L_2, two capacitors are C_1 and C_2. i_{C1}, i_{C2} and i_{L1}, i_{L2} are the respective currents flowing through C_1, C_2 and L_1, L_2. v_{C1}, v_{C2}, v_{L1} and v_{L2} are the respective large signal voltages across C_1, C_2 and L_1, L_2. i_0 and v_0 are the large signal current and voltage respectively at load resistance. Any combination of inputs can be used to operate the suggested converter. To see the converter in action, assume that V_1 is greater than V_2. The switches S_1 to S_4 respective switching frequencies are f_{S1} to f_{S4} and assuming $f_{S1}= f_{S2}= f_{S3}= f_{S4} =1/T$ The suggested work does not account for solar panel leakage current, fuel cell dynamics, or sunlight's erratic nature. The entire functioning of the planned converter is covered in sections II.1.1 to II.1.6, together with the corresponding mathematical equations.

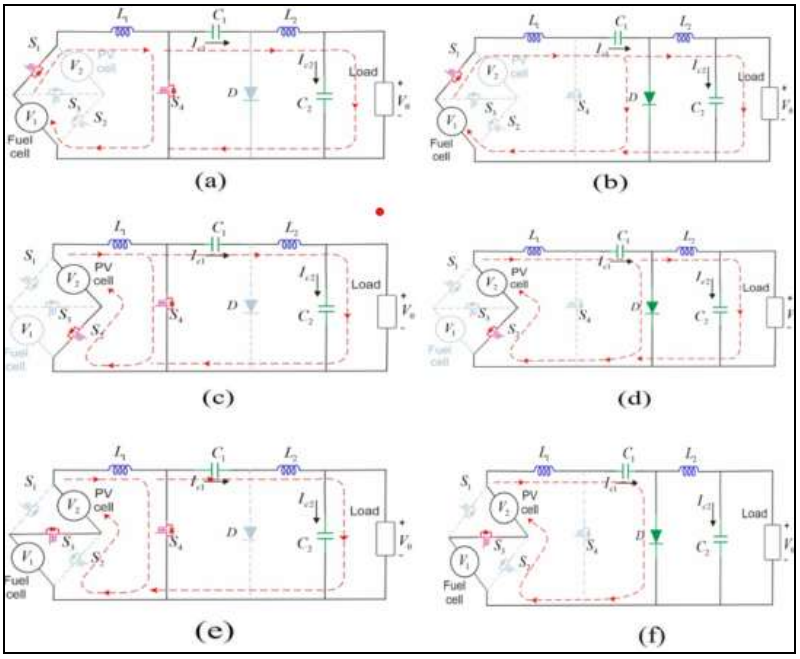

Figure 3: Modes of operation. a. Mode (1), b. Mode (2), c. Mode (3), d. Mode (4), e. Mode (5), and f. Mode (6).
Source: Authors, (2025).

II.1.1 First Mode: In the Mode-1 S_1, S_4 are ON state and S_2, S_3 and D are OFF state. The Fig. 3 (a) shows the First Mode circuit by using KCL and KVL on mode 1 circuit.

$$v_{L1} = v_1 \tag{1}$$
$$v_{L2} = -v_{C1} - v_{c2} \tag{2}$$
$$i_{L1} = i_1 \tag{3}$$
$$i_{L2} = i_{C1} \tag{4}$$
$$i_0 = i_2 - i_{C2} \tag{5}$$
$$v_0 = v_{C2} = i_0 R = -i_{C2} R \tag{6}$$

II.1.2 Second Mode:

In the second Mode the switches S_1 , D are in turn ON and S_2, S_3 and S_4 are in OFF state. The corresponding circuit under this mode is shown in Figure. 3(b)
The equations from (7) to (10) can be obtained by using KCL and KVL.

$$v_{L1} = v_1 - v_{C1} \tag{7}$$
$$v_{L2} = -v_0 \tag{8}$$
$$i_{L1} = i_{C1} \tag{9}$$
$$i_{L2} = i_0 + i_{C2} \tag{10}$$

II.1.3 Third Mode:

In this mode, S_2, S_4 are ON and D, S_1 and S_3 OFF state. The Figure. 3 (c) shows the equivalent circuit.
The equations from (11) to (16) can be obtained by using KCL and KVL.

$$v_{L1} = v_2 \tag{11}$$
$$v_{L2} = -v_{C1} - v_{C2} \tag{12}$$
$$i_{L1} = i_1 \tag{13}$$
$$i_{L2} = i_{C1} \tag{14}$$

$$i_0 = i_2 - i_{C2} \tag{15}$$

$$v_0 = v_{C2} = i_0 R = (i_2 - i_{C2})R \tag{16}$$

II.1.4 Forth Mode: Fourth mode, S_2, D are ON and S_1, S_3 and S_4 are OFF state. The Figure. 3 (d) shows the equivalent circuit. The equations from (17) to (20) can be obtained by using KCL and KVL

$$v_{L1} = v_2 - v_{C1} \tag{17}$$

$$v_{L2} = -v_0 \tag{18}$$

$$i_{L1} = i_{C1} \tag{19}$$

$$i_{L2} = i_0 + i_{C2} \tag{20}$$

II.1.4 Fifth Mode: In fifth Mode, S_3, S_4 are ON and S_1, S_2 and D are OFF state. The Figure. 3 (e) shows the under fifth mode.

The equations from (21) to (26) can be obtained by using KCL and KVL.

$$v_{L1} = v_1 + v_2 \tag{21}$$

$$v_{L2} = -v_{C1} - v_{C2} \tag{22}$$

$$i_{L1} = i_1 \tag{23}$$

$$i_{L2} = i_{C1} \tag{24}$$

$$i_0 = i_2 - i_{C2} \tag{25}$$

$$v_0 = v_{C2} = i_0 R \tag{26}$$

II.1.6 Sixth Mode: In Mode six, the S_3, D are in ON state and S_1, S_2 and S_4 are in OFF state. The Figure. 3 (f) shows the corresponding circuit.

by using KCL and KVL the equations (27) to (30) can be obtained.

$$v_{L1} = v_1 + v_2 - v_{C1} \tag{27}$$

$$v_{L2} = -v_0 \tag{28}$$

$$i_{L1} = i_{C1} \tag{29}$$

$$i_{L2} = i_0 + i_{C2} \tag{30}$$

II.2 STATE-STATE MODELLING

To determine the relationship between output current and voltage in terms of the duty cycle, as well as the expressions for the values of inductors and capacitors, steady-state modelling is essential. With help of (1) to (30), equations

$$V_0 = -\frac{d_1+d_3+d_5}{1-d_1-d_3-d_5}\left(V_1(1-d_3-d_4) + V_2(1-d_1-d_2)\right) \quad (31)\ I_{L2} = I_0 = \frac{V_0}{R}\ (32)\ I_{L1} = \frac{-V_0}{R}\frac{d_1+d_3+d_5}{1-d_1-d_3-d_5} \tag{33}$$

System performance is determined by the design and selection of inductors and capacitors, which also enable the converter to operate in the necessary conduction mode. the value of the inductors and capacitor equations are

$$L_1 = \frac{(V_1+V_2)d_5T}{\Delta I_{L1}} \tag{34}$$

$$L_2 = \frac{V_0 d_5 T}{\Delta I_{L2}} \tag{35}$$

$$C_1 = \frac{V_0 d_5 T}{R\Delta V_{C1}} \tag{36}$$

$$C_2 = \frac{V_0 d_5 T}{R\Delta V_{C2}} \tag{37}$$

III. EFFICIENCY

Power converter's efficiency is mostly affected by parasitic components. The recommended converter's power loss is shown below.

$$Power\ loss\ due\ to\ the\ internal\ elements = P_{S1} + P_{S2} + P_{S3} + P_{S4} + P_{RL1} + P_{RL2} + P_{RC1} + P_{RC2} + P_{RD} + P_{VFD}$$
$$= {I_{S1R}}^2 R_{S1} + {I_{S2R}}^2 R_{S2} + {I_{S3R}}^2 R_{S3} + {I_{S4R}}^2 R_{S4} + {I_{L1R}}^2 R_{L1} + {I_{L2R}}^2 R_{L2} + {I_{C1R}}^2 R_{C1} + {I_{C2R}}^2 R_{C2} + {I_{DR}}^2 R_D + I_{Davg} V_{FD}$$

The suggested converter's overall power loss is,

$$P_{Loss} = Power\ loss\ due\ to\ the\ parasitic\ elements + Switching\ losses + Inductor\ core\ losses$$

Therefore, the efficiency of the converter is,

$$\%Efficiency = \frac{P_{out}}{P_{out} + P_{Loss}} \times 100$$

The converter offers great efficiency and accuracy at specified inputs and duty cycles.

IV. CASE STUDIES

As indicated in Table 1, the MIC has six operating modes in addition to three distinct methods for controlling the input and output powers and voltages. the duty ratio of switch S4 is D4 and similarly, the duty cycle of switches S_1, S_2 and S_3 are D_1, D2 and D_3 respectively

Table 1: Possible operating situations of the power converter.

Cases	Fuel cell (V_1)	Solar panel (V_2)	Action	O/P Voltage (V_0)
1	1	0	Considering Fuel cell	$\frac{V_1 D_4}{1-D_4}$; $D_1 = 1$
2	0	1	Considering PV cell	$\frac{V_2 D_4}{1-D_4}$; $D_2 = 1$
3	1	1	Considering Fuel cell and PV cell together.	$\frac{(V_1 + V_2) D_4}{1-D_4}$ $D_3 = 1$

Source: Authors, (2025).

IV.1 FUEL CELL ALONE

Table 1 illustrates that in case 1, the fuel cell alone can provide the necessary power to the load using the suggested converter. The vehicle will be able to run in the lack of sunshine under this hypothetical operating situation.

IV.2 SOLAR PV CELL ALONE

Table 1 illustrates that in case 2, the proposed converter can provide the necessary power to the load using only a solar PV cell. In this hypothetical situation, the vehicle will be able to run solely on sunshine. The vehicle will use less hydrogen as a result of this process, resulting in nearly zero operating costs.

IV.3 BOTH FUEL CELL AND SOLAR PV CELL

Table 1 illustrates how the proposed converter can use a fuel cell and a PV cell to help the load receive the necessary electricity. Under this hypothetical set of conditions, the vehicle will be able to run on hydrogen and sunlight. In this case, the converter will come in when the solar PV panel isn't able to give the load the necessary amount of electricity on its own. This process will assist the vehicle in using less hydrogen, which will lower the vehicle's operating costs.

IV. RESULTS AND DISCUSSIONS

This article presents the mathematical modelling of a Cuk-based multi-input converter and analyses its steady-state behaviour. The performance of the proposed converter is validated through an experimental setup.

Figure 4: Experimental setup of CUK based novel multi-input converter.
Source: Authors, (2025).

Table 2: Experimental setup of CUK converter parameters.

Parameter	Value
I/P Voltages	$V_1 = 20V$, $V_2 = 12V$
O/P Voltage	$V_0 = 48V$
O/P Power	$P_0 = 250W$
Switching Frequency	10 KHz
Duty Cycle $D_1 = D_2 = D_3$	0.33
Duty Cycle D_4	0.72
Inductors	$L_1 = 24mH, L_2 = 50mH$
Capacitors	$C_1 = 750\mu F$, $C_2 = 750\mu F$
MOSFETs (4)	FQA38N30
Diode	MUR1560
Load	$R = 10\Omega$

Source: Authors, (2025).

The switching frequency is $f_s = 10kHz$. The PV cell voltage is $V_2 = 12V$ and the fuel cell voltage is $V_1 = 20V$ respectively. The suggested converter was anticipated to generate 48V in order to supply 250W at the output terminal. The suggested converter's experimental setup is depicted in Figure. 4, and Table 2 lists the parts and setup parameters that were chosen. Experimentally gerenated switching pulses of the four MOSFET switchesV_{GS1}, V_{GS2}, V_{GS3} and V_{GS4} are shown in Figure. 5(a). The switching frequencies of S_1, S_2 and S_3, S_4 are almost identical, which is equal to 10KHz.The proto type model waveforms of inductor currents I_{L1} and I_{L2} and capacitor voltages V_{C1}, V_{C2} are shown in Figure. 5(b). The dc root mean square values of I_{L1}, I_{L2} and V_0 are 18.19 A, 6.38 A and 56.32 V, 47.74 V respectively.

The voltage across the swithes are V_{GS1}, V_{GS2}, V_{GS3} and V_{GS4} are shown in Figure. 5(c). The voltage stress values of S_1, S_2 and S_3, are almost less than or equal to the highest input voltage and stress on voltage value of S_4 is lower than the 2 times of V_0. The input voltages V_1 , V_2 and output voltage and current V_0, I_0 waveforms are shown in Figure. 5(d). The values of input voltages V_1, V_2 and output voltage V_0 and output current I_0 are 20 V, 12V and 47.74 V, 6.36A respectively. The proposed converter delivers power to the load at a high efficiency of 96.4%, compare to other converters are mentioned in table.3

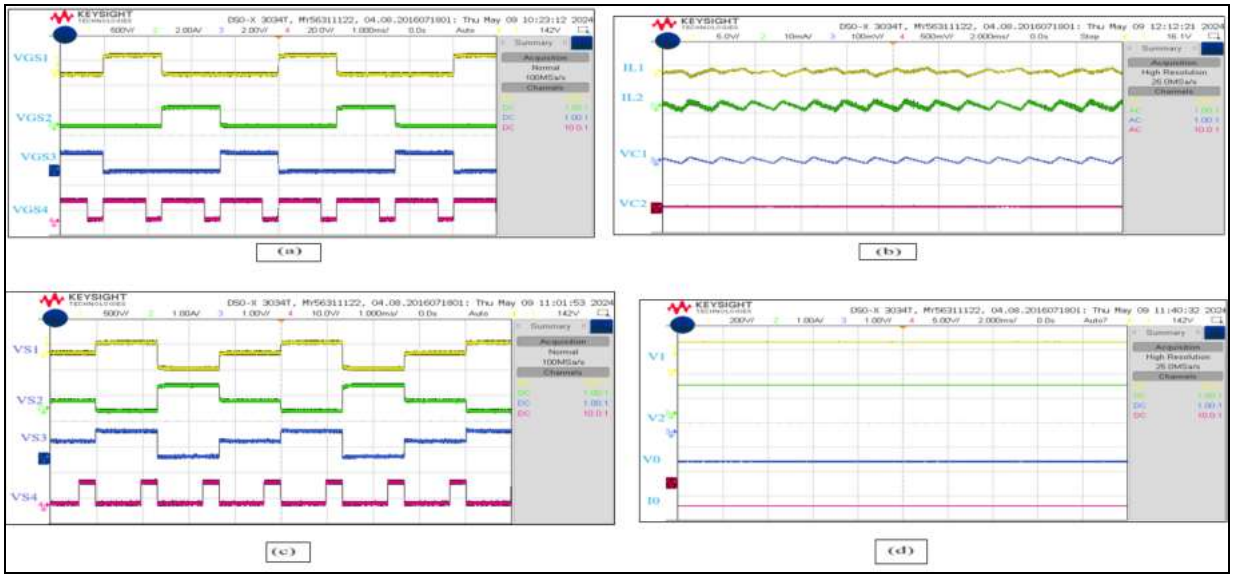

Figure 5: The proto type model experimental waveforms. (a) Pulses of S_1, S_2 and S_3 and S_4. (b) Inductor currents and Capacitor voltages. (c) voltage stress of S_1, S_2 and S_3, S_4 switches. (d) Input and output voltages and output current.
Source: Authors, (2025).

Table 2: Comparing the proposed converter against existing converters topologies.

Topology	[15]	[16]	[17]	[18]	[19]	[20]	[21]	[22]	[23]	Proposed
Gain	A_{11}	A_{12}	A_{13}	A_{14}	A_{15}	A_{16}	A_{17}	A_{17}	A_{18}	A_{19}
Number of sources	2	2	2	2	3	2	2	2	2	2
Number of uni-directional switches	0	4	0	2	4	6	4	3	4	4
Number of capacitors	2	1	1	1	1	4	4	3	4	2
Number of inductors	2	1	1	1	1	4	4	3	4	2
Numbers of Bi-directional power switches	3	0	3	2	2	2	0	0	1	0
No. of diodes	5	3	1	0	2	2	4	3	1	1
No. of relays	0	4	3	0	0	0	0	0	0	0
Stress on Voltage	High	-	-	High	Low	High	Moderate	Moderate	Moderate	Low
% Efficiency	93.50	94	93	94	88-94	91	95	94	95	96.4

Source: Authors, (2025).

$$A_{11} = V_0 = \frac{(d_1+d_2)V_1+d_2V_2}{1-d_1-d_2} \qquad A_{12} = V_0 = \frac{d_1V_1+d_2(V_1+V_2)+d_3V_2}{1-d_1-d_2-d_3}$$

$$A_{13} = V_0 = \frac{d_1V_1+(1-d_1)V_2}{1-d_2} \qquad A_{14} = V_0 = -\frac{d_1V_1+d_2V_2+d_3(V_1+V_2)}{1-d_1-d_2-d_3}$$

$$A_{15} = V_0 = \frac{d_1V_{battery}+(1-d_1)V_1+(1-d_2)V_2}{1-d_3} \qquad A_{17} = V_0 = \frac{(2-d_1)V_1+V_2}{(1-d_1)^2}$$

$$A_{18} = V_0 = \frac{(\,d_1 - 2d_2 + d_1d_2}{(1-d_1)^2(d_1-d_2)}\,V_1 + \frac{d_2(1-d_1)}{d_1(d_1-d_2)}V_2 A_{19} = V_0 = -\frac{d_1+d_3+d_5}{1-d_1-d_3-d_5}\big(V_1(1-d_3-d_4)+V_2(1-d_1-d_2)\big)$$

V. CONCLUSIONS

The modelling of the inimitable MIC with high voltage gain for hybrid electric vehicles (HEVs) drives has been clearly demonstrated and verified by this work. With this design, the load might receive energy continuously from two inputs. Furthermore, the idea of using various switching frequencies has been implemented well, resulting in substantial control over power flow and terminal voltage. The steady-state modelling of the proposed converter are established in order to achieve accurate modelling with improved inspection of the converter.. The literature compares the efficiency of the proposed power converter with existing power converters that are currently on the market. At the intended load, the suggested converter shows 96.4% efficiency, and there is also less stress on the semiconductor switches. Gains and efficiency are outstanding, and losses are negligible. Especially this converter is suitable for EV application.

VI. AUTHOR'S CONTRIBUTION

Conceptualization: Author One, Author Two.
Methodology: Author One and Author Two.
Investigation: Author One and Author Two.
Discussion of results: Author One, Author Two.
Writing – Original Draft: Author One.
Writing – Review and Editing: Author One and Author Two.
Resources: Author one.
Supervision: Author Two.
Approval of the final text: Author One, Author Two.

VII. REFERENCES

[1] M. Adnan, D. Ibrahim, Hydrogen as a renewable and sustainable solution in reducing global fossil fuel consumption, International Journal of Hydrogen Energy 33(16) (2008) 4209-4222. https://doi.org/10.1016/j.ijhydene.2008.05.024.

[2] The National Academy of Science Engineering Medicine, Our energy resources - fossil fuels, The National Academy of Science Engineering Medicine. http://needtoknow.nas.edu/energy/energy-sources/fossil-fuels/, 2021 (accessed 2 November 2021).

[3] R. Robert, Fossil fuels still supply 84 percent of world energy - and other eye openers from BP's annual review. Forbes. https://www.forbes.com/sites/rrapier/2020/06/20/bp-review-new-highs-in-global-energy-consumption-and-carbon-emissions-in-2019/?sh=66d08ad166a1, 2019 (accessed 20 July 2021).

[4] R. Hannah, R. Max, Energy production and consumption, Our World in Data. https://ourworldindata.org/energy-production-consumption, 2021 (accessed 8 November 2021).

[5] U.S Energy Information Administration, Energy and the environment - where greenhouse gases come from. https://www.eia.gov/energyexplained/energy-and-the-environment/where-greenhouse-gases-come-from.php, 2021 (accessed 21 October 2021).

[6] B. Eisavi, F. Ranjbar, H. Nami, A. Chitsaz, Low-carbon biomass-fueled integrated system for power, methane and methanol production, Energy Conversion and Management 253 (2022) 115163-115185. https://doi.org/10.1016/j.enconman.2021.115163.

[7] Y. Budak, Y. Devrim, Comparative study of PV/PEM fuel cell hybrid energy system based on methanol and water electrolysis, Energy Conversion and Management 179 (2019) 46-57. https://doi.org/10.1016/j.enconman.2018.10.053.

[8] A.M. Amr, A.I.M. Yasser, Extracting and defining flexibility of residential electrical vehicle charging loads, IEEE Transactions on Industrial Informatics 14(2) (2018) 448-461. https://doi.org/10.1109/TII.2017.2724559.

[9] S. Bairabathina, S. Balamurugan, Review on non-isolated multi-input step-up converters for grid-independent hybrid electric vehicles, International Journal of Hydrogen Energy 45(41) (2020) 21687-21713. https://doi.org/10.1016/j.ijhydene.2020.05.277.

[10] C.E. Thomas, Fuel cell and battery electric vehicles compared, International Association for Hydrogen Energy 34(15) (2009) 6005-6020. https://doi.org/10.1016/j.ijhydene.2009.06.003.

[11] G. Nicoletti, N. Arcuri, G. Nicoletti, R. Bruno R. A technical and environmental comparison between hydrogen and some fossil fuels, Energy Conversion and Management 89 (2015) 205-213. https://doi.org/10.1016/j.enconman.2014.09.057.

[12] T. Capurso, M. Stefanizzi, M. Torresi, S. M. Camporeale, Perspective of the role of hydrogen in the 21st century energy transition, Energy Conversion and Management 251 (2022) 114898-114914. https://doi.org/10.1016/j.enconman.2021.114898.

[13] International Energy Agency, The future of hydrogen, International Energy Agency. https://www.iea.org/reports/the-future-of-hydrogen, 2019 (accessed 05 May 2020).

[14] Alternative Fuels Data Center, Hydrogen production and distribution, U.S Department of Energy. https://afdc.energy.gov/fuels/hydrogen_production.html, 2021 (accessed 24 June 2021).

[15] K. H. Saeideh, T. Sajjad, R.F. Mohammad, S. Mehran, Design and analysis of a novel SEPIC-based multi-input DC/DC converter, IET Power Electronics 10(12) (2017) 1393-1402. https://doi.org/10.1049/iet-pel.2016.0654.

[16] S. Kumaravel, G.G. Kumar, V. Kuruva, V. Karthikeyan, Novel non-isolated modified interleaved DC-DC converter to integrate ultracapacitor and battery sources for electric vehicle application, 20th National Power Systems Conference (NPSC) (2018). https://doi.org/10.1109/NPSC.2018.8771810.

[17] G. K. Gangavarapu, S. Kumaravel, A. Sivaprasad, K. Venkitusamy, Dual input superboost DC–DC converter for solar powered electric vehicle, IET Power Electronics 12(9) (2019) 2276-2284. https://doi.org/10.1049/iet-pel.2018.5255.

[18] A. Sivaprasad, G.K. Gangavarapu, S. Kumaravel, S. Ashok, A non-isolated bridge-type DC–DC converter for hybrid energy source integration, IEEE Transactions on Industry Applications 55(4) (2019) 4033-4043. https://doi.org/10.1109/TIA.2019.2914624.

[19] K. Varesi, S. H. Hosseini, M. Sabahi, E. Babaei, Performance analysis and calculation of critical inductance and output voltage ripple of a simple non-isolated multi-input bidirectional DC-DC converter, International Journal of Circuit Theory and Applications 46(3) (2018) 543-564. https://doi.org/10.1002/cta.2392.

[20] K. Varesi, S. H. Hosseini, M. Sabahi, E. Babaei, S. Saeidabadi, N. Vosoughi, Design and analysis of a developed multiport high step-up DC–DC converter with reduced device count and normalized peak inverse voltage on the switches/diodes, IEEE Transactions on Power Electronics 34(6) (2018) 5464-5475. https://doi.org/10.1109/TPEL.2018.2866492.

[21] K. Varesi, S. H. Hosseini, M. Sabahi, E. Babaei, Modular non isolated multi-input high step-up DC–DC converter with reduced normalized voltage stress and component count, IET Power Electronics 11(6) (2018) 1092-1100. https://doi.org/10.1049/iet-pel.2017.0483.

[22] K. Varesi, S. H. Hosseini, M. Sabahi, E. Babaei, A high-voltage gain nonisolated noncoupled inductor based multi-input DC-DC topology with reduced number of components for renewable energy systems, International Journal of Circuit Theory and Applications 46(3) (2018) 505-518. https://doi.org/10.1002/cta.2428.

[23] Gaurav, N. Jayaram, S. Halder, K. P. Panda and S. V. K. Pulavarthi, "A Novel Design With Condensed Component of Multi-Input High Gain Nonisolated DC–DC Converter for Performance Enhancement in Carbon Neutral Energy Application," in IEEE Journal of Emerging and Selected Topics in Industrial Electronics, vol. 4, no. 1, pp. 37-49, Jan. 2023, doi: 10.1109/JESTIE.2022.3211779.